CrystEngComm

Accepted Manuscript

ROYAL SOCIETY OF CHEMISTRY

www.rsc.org/crystengcomm

Journal Name

ARTICLE

Water-induced phase transformation of a Cu^{II}-coordination framework with pyridine-2,5-dicarboxylate and di-2-pyridyl ketone: synchrotron radiation analysis

Received 00th January 20xx,
Accepted 00th January 20xx

DOI: 10.1039/x0xx00000x

www.rsc.org/

Francisco Llano-Tomé,[a] Begoña Bazán,[a,b*] M. Karmele Urtiaga,[a] Gotzone Barandika,[c] Arkaitz Fidalgo-Marijuan,[a] Roberto Fernández de Luis,[a,b] and María I. Arriortua[a,b]

Phase transformations in solid coordination frameworks (SCFs) are of interest for several applications, and this work reports on a crystal-to-crystal transformation found for a hydrogen bonded Cu^{II}-based solid coordination frameworks (SCF). Thus, combination of PDC and $(py)_2C(OH)_2$ ligands, where PDC is pyridine-2,5-dicarboxylate and $(py)_2C(OH)_2$ is the derivative gem-diol of di-2-pyridyl ketone ($(py)_2CO$), produces $[Cu(PDC)((py)_2C(OH)_2)(H_2O)]$ (**1**). Compound **1** transforms into $[Cu(PDC)((py)_2C(OH)_2)]$ (**2**) by thermally-induced dehydration. Characterization of both compounds has been carried out by means of IR spectroscopy, single crystal and powdered sample X-ray diffraction (XRD) through conventional and synchrotron radiation, thermogravimetry (TG), X-ray thermodiffractometry (TDX), and scanning electron microscopy (SEM). Since the molecules of water in **1** are coordinated to the metal ions, their removal provokes local distortions on the coordination sphere (square pyramidal for **1** and square planar for **2**), which extend through the whole framework affecting the hydrogen bond system and the packing. In fact, the wavy nature of the planes in **1** becomes sharper in **2**, producing an oscillation of the framework: i.e., from open (**1**) to close (**2**) waves. The crystal-to-crystal transformation is reversible (**1**↔**2**) and hysteresis has been observed associated to it. Quantum-mechanical calculations based on the density functional theory (DFT) show that the **1**↔**2** structural rearrangement involves a high amount of energy, meaning that the role of the coordinated molecule of water exceeds the mere formation of hydrogen bonds.

Introduction

Crystal engineering of solid coordination frameworks (SCFs)[1-4] has showed a lot of interest along the last decade, not only for their potential applications as functional materials in gas storage,[5-7] gas separation,[8-10] heterogeneous catalysis,[11-13] drug delivery,[14-16] chemical sensing,[17,18] nonlinear optics[19] and biomedical imaging,[20,21] but also for their fascinating variety of structural topologies and flexible behavior to external stimuli.[22,23] Thus, many interesting solid-state transformations[24] of SCFs can be induced by light, heat, guest removal, uptake or exchange, expansion or reduction of the coordination sphere, oxidation of metal centers, condensation, or reactions between the ligands.[25,26]

Referred to changes in the coordination sphere, it is worth noticing that removal/uptake of a ligand can provoke local distortions that can extend along the whole framework. When the latter occurs, in order to keep crystalline integrity (*i.e.* in order to avoid the collapse of the framework), appropriate additional ligands must be used. These additional ligands must assume the necessary structural rearrangement affecting not only local distortions on secondary building units (SBUs) but also those affecting the inter-SBU cohesion.

Among the vast variety of organic ligands that can be used for SCFs, polycarboxilates (like PDC) and dipyridylic (like ($(py)_2CO$) are good candidates. The PDC ligand is the divalent anion of pyridinedicarboxylic acid (H_2PDC, Scheme 1). It is non-centrosymmetric and exhibits five potential donor atoms which produce a large variety of possible bond fashions. In fact, up to twenty three coordination modes have been reported for this ligand, and we first reported four of them.[27-31] On the other hand, di-2-pyridyl ketone ($(py)_2CO$), also abbreviated as dpk in the literature (Scheme 1), can be *in situ* transformed into a new specimen in an aqueous medium through nucleophilic attack on the keto group in the presence of metal ions.[32-38] The derivative *gem*-diol $(py)_2C(OH)_2$ can coordinate to the metal ion as neutral molecule or monovalent anion.

In this sense, we previously reported on the PDC-$(py)_2C(OH)_2$ combination of ligands.[29,30] In fact, the host-guest chemistry of Ni^{II}-PDC-$(py)_2C(OH)_2$ compounds is characterized by the exchange of solvents associated to reversible crystal-to-

[a] Departamento de Mineralogía y Petrología, Facultad de Ciencia y Tecnología, Universidad del País Vasco (UPV/EHU), Barrio Sarriena s/n, 48940 Leioa, Bizkaia.
[b] BCMaterials Parque Tecnológico de Zamudio, Ibaizabal Bidea, Edificio 500–Planta 1, 48160, Derio, Spain.
[c] Departamento de Química Inorgánica, Facultad de Ciencia y Tecnología,
Electronic Supplementary Information (ESI) available: ORTEP detail of the structures, IR spectra, thermogravimetry and distortion diagrams of coordination spheres for metal complexes, Rietveld Refinement of compound **2**, X-ray thermodiffractometry, crystallographic data and CIF files. CCDC 1059613 (compound **1**) and 1059614 (compound **2**). See DOI: 10.1039/x0xx00000x

amorphous transformations, and their reversibility accredits the use of this system as a solvent sensor (patent WO2013057350 A1).[30] As far as we are concerned, no further M-PDC-$(py)_2C(OH)_2$ systems have been explored to date, so we decided to investigate the combination for M=Cu^{II}.

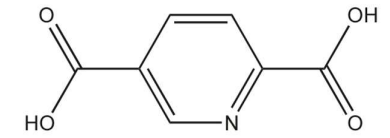

2,5-pyridinedicarboxylic acid (H_2PDC)

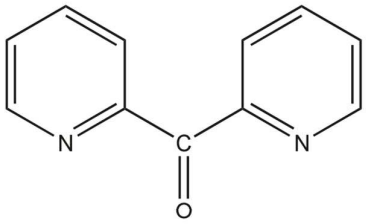

Di-2-pyridyl ketone $(py)_2CO$

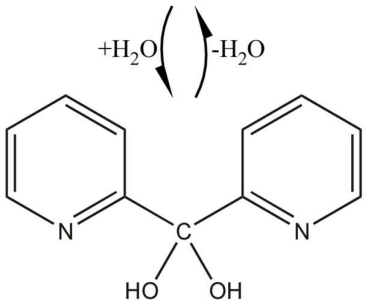

gem-diol form $(py)_2C(OH)_2$

Scheme 1. Lewis structure for H_2PDC, $(py)_2CO$ and $(py)_2C(OH)_2$.

Selection of Cu^{II} is based on some outstanding, phase transformations found in literature. In fact, Díaz-Gallifa *et al.*[39] prepared five Cu^{II}–Ln^{III} heteronuclear metal–organic frameworks $[Ln_4Cu_4(H_2O)_n(bta)_5]\cdot mH_2O$ (H_4bta=1,2,4,5-benzenetetracarboxylic acid, n=24,26 and m=14-22). The noticeable fact is that, even if the amount of water molecules in the frameworks is very high, the transformation from expanded to shrinking phases only occurs in a dry atmosphere. On the other hand, Yang *et al.*,[40] reported on the influence of the solvent and the coordination sphere on the conformation of some 1D Cu^{II}-based coordination polymers in which the removal/adsorption of water molecules provokes the formation of different isomers. Washizaki *et al.*,[41] prepared a Cu^{II}-based SCF where dimeric SBUs form a supramolecular array stabilized through π-π interactions. A reversible crystal transformation was found involving reversible apical-ligand substitution at the copper centres upon hydration–dehydration. Jiang *et al.*[42] reported another outstanding single-crystal to single-crystal transformation taking place upon removal of the noncoordinated water in an ionic net exhibiting cationic and anionic Cu^{II}-complexes and affecting the π-π and hydrogen bond system. Finally, we have reported recently on the crystal-to-crystal transformation of the ionic net $[Cu((py)_2C(OH)_2)_2](H_2bta)$[43] where dehydration of the coordinated molecules and counter-anions is involved. Therefore, with the exception of the transformations observed for Cu^{II}–Ln^{III} heteronuclear metal-organic frameworks,[39] the rest of them are water-related.

Taking into account the above mentioned aspects, we have explored the Cu^{II}-PDC-$(py)_2C(OH)_2$ system, and this work reports on the synthesis, crystal structure and thermal stability of $[Cu(PDC)((py)_2C(OH)_2)(H_2O)]$ (**1**) and $[Cu(PDC)((py)_2C(OH)_2)]$ (**2**). Both compounds have been analyzed by means of IR spectroscopy, X-ray diffractometry (XRD) on single crystal and powdered samples (including conventional and synchrotron radiation), scanning electron microscopy (SEM), thermogravimetry (TG), and X-ray thermodiffractometry (TDX). Quantum mechanics calculations have been also carried out by means of the density functional theory (DFT). The interest of this work lies on the fact that we have found a reversible **1**↔**2** transformation that is induced by a single molecule of coordinated water (per metal ion), provoking a rearrangement of the system which involves a high energy exchange.

Experimental section

General

All solvents and chemicals were used as received from reliable commercial sources. The reactants 2,5-pyridinedicarboxylic acid (H_2PDC), di-2-pyridyl ketone ($(py)_2CO$), copper(II) nitrate hydrate 99%, and agarose were purchased from Sigma-Aldrich Co.

Synthesis of $[Cu(PDC)((py)_2C(OH)_2)(H_2O)]$ (1)

H_2PDC (16.4 mg, 0.1 mmol), $(py)_2CO$ (18.4 mg, 0.1 mmol) and agarose (100 mg) were dropped in a test tube and dissolved in a water solution (10 mL) after stirring and heating (50°C) in a bain-marie. Once reached 50°C, the temperature was increased slowly until 90°C, maintaining it constant during 20 minutes. Finally, the solution was cooled slowly until 65°C, and two drops of NaOH (1M) were added to the solution. The agarose gel was formed after ten minutes.

On the other hand, $Cu(NO_3)_2\cdot 2.5H_2O$ (37.3 mg, 0.2 mmol) was dissolved in a water solution (5 mL) and added slowly above the gel. After two days, blue prismatic crystals were obtained. The sample was washed and dried with ethanol, collecting single crystals for X-ray diffraction experiment. The density was measured by the flotation method[44] in a mixture of bromoform/chloroform. Experimental value is 1.68(4) $g\cdot cm^{-3}$.

Elemental analysis: Found: C, 48.2(3); H, 3.1(2); N, 9.2(2). Calc. For $C_{18}H_{15}N_3O_7Cu$: C, 48.12; H, 3.34; N, 9.35. IR: ν_{max}/cm^{-1} 3470 (OH), 1656 and 1604 (aroC-C), 1557 (asCOO), 1390, 1364 and 1453 (sCOO), 1282 (C-N), 826, 774 and 693 (C-H) and 548-514 (Cu-N) (Figure S1, ESI†)).

Formation of [Cu(PDC)((py)$_2$C(OH)$_2$)] (2)

Formation of compound **2** was carried out by thermal treatment of **1**. Further details will be discussed in the section "Thermal analysis and structural transformation".

Single-crystal X-ray diffraction for [Cu(PDC)((py)$_2$C(OH)$_2$)(H$_2$O)] (1)

Prismatic single-crystal of compound **1** with dimensions given in Table 1 was selected under polarizing microscope and mounted on MicroMounts™. Single-crystal data were collected at 100 K on an Agilent Technologies Supernova single source diffractometer with Cu-Kα radiation (1.54184 Å). Details of the crystal data and some features of the structure refinement are reported in Table 1, and selected bond length and angles are listed in Tables S1 and S2 (ESI†).

Lattice constants were obtained by using a standard program belonging to the diffractometer software, confirming at the same time the good quality of the single-crystals.[45] The Lorentz polarization and absorption corrections were made with the diffractometer software, taking into account the size and shape of the crystals. The structure was solved by direct methods using SIR92[46] program, with the orthorhombic *Pbca* space group, which allowed us to obtain the positions of the copper atom, as well as the oxygen and nitrogen atoms and some of the carbon atoms of both PDC and (py)$_2$C(OH)$_2$ ligands.

The refinement of the crystal structure was performed by full-matrix least-squares based on F^2, using the SHELXL-97[47] program, obtaining the remaining carbon atoms and allowing the allocation of the hydrogen atoms. Anisotropic thermal parameters were used for all non-hydrogen atoms. The hydrogen atoms belonging to the organic molecules were fixed geometrically, allowed to ride on their parent carbon atoms (C-H 0.95 Å), and were refined with common isotropic displacements. The position of the hydrogen atoms bonded to the coordinated water molecule, were fixed using DFIX and DANG instructions in the refinement to adjust the O-H distance to 0.82 Å and the H-O-H angle to 112°, respectively. ORTEP image of the asymmetric unit for **1** can be seen in Figure S2, ESI†.

Table 1. Details of the crystal data, structural resolution and refinement procedure for **1** (single crystal X-ray diffraction).

Compound **1**	[Cu(PDC)((py)$_2$C(OH$_2$))(H$_2$O)]
Formula	$C_{18}H_{15}N_3O_7Cu$
FW, g·mol^{-1}	448.87
Crystal system	Orthorhombic
Space group (no. 61)	*Pbca*
a, Å	7.2953(2)
b, Å	17.2658(5)
c, Å	28.4236(7)
V, Å ^{3}	3580.2(2)
Z	8
ρ_{obs}, ρ_{cal}, g·cm^{-3}	1.68(5), 1.666
F(000)	1832
μ, mm^{-1}	2.178
Crystal size, mm	0.033 x 0.032 x 0.019
Absorption correction	Multy-scan
Radiation, λ, Å	1.54184
Temperature, K	100(2)
Reflections collected, unique	19752, 3272 (R_{int}=0.0646)
Limiting indices	-7<=h<=8
	-20<=k<=18
	-34<=l<=34
Refinement method	Full-matrix least-squares on F^2
Final *R* indices [I > 2σ(I)][a]	R1 = 0.0390, wR2 = 0.1032
R indices (all data)[a]	R1 = 0.0494, wR2 = 0.1122
Goodness of fit on F^2	0.855
Parameters / restraints	268 / 3

[a]R1=[(|F$_0$|- |F$_c$|)]/|F$_0$|. wR2=[[w|F$_0$|^2-|F$_c$|^2)^2]/[w(|F$_0$|^2)^2]$^{1/2}$

X-Ray Powder Diffraction (XRPD) for [Cu(PDC)((py)$_2$C(OH)$_2$)] (2).

A powdered crystalline sample of compound **2** was formed by transformation of **1**, as explained in the thermal stability section. The powder pattern of the sample at 130°C was collected in the BM25B Spline of the ESRF (European Synchrotron Radiation Facility). The powdered sample was introduced in a 1 mm capillary and the wavelength set at 0.8276(2) Å. The pattern was recorded from 3.5 to 40.24° in 2ϑ (°), with a step of 0.01° and 2s per point.

In the initial steps of the refinement, the profile matching analysis allowed us to determinate the cell parameters and to refine the profile variables. The structural model obtained for compound **1** was used as the starting point for the structural refinement of **2** using JANA2006[48] program. Rigid bodies were constructed for the pyridyl rings and the carboxylate groups of the ligands. The bond distances between rigid bodies were restrained to usual values, for example for the C–C and C–N bonds of the PDC and (py)$_2$C(OH)$_2$ pyridyl rings a distance restraint of 1.39Å with 0.001sd was imposed, and for the Cu–N and Cu1–O bonds between the PDC, (py)$_2$C(OH)$_2$ and Cu^{II} typical values between 1.93 Å and 2.097 Å with 0.05sd were used. Torsion angles for both ligands were also restrained to usual values.

First, each rigid body orientation and translation was refined separately until the refinement achieved the convergence. In a second step of the refinement the pyridyl groups were refined

jointly. In the last step, all the rigid bodies, including the carboxylic groups, were refined at the same time.

In that point of the refinement, the rigid bodies of the PDC and pyridyl rings, including the carboxylic groups of both ligands, were set free and the copper, oxygen and nitrogen atoms were refined independently, but introducing several bond distance and angle restraints, in order to maintain the general shape of the square-planar geometry. The bond valance values were checked routinely during the refinement, introducing progressively more chemical logic bond distance restraints. Common isotropic thermal parameters were used for the copper, oxygen, carbon and nitrogen atoms. In the last steps of the refinement, the hydrogen atoms belonging to the PDC and $(py)_2C(OH)_2$ ligands were geometrically introduced, and the angles regarding the linkage between the pyridyl ring and the carboxylic groups of the PDC ligand were also restrained.

A large number of restrains were used during the refinement, but most of them are related with the rigid pyridyl groups belonging to the organic ligands.

Details of the crystal data and some features of the structure refinement are reported in Table 2. ORTEP image of the asymmetric unit for **2** can be seen in Figure S3, ESI† and Tables S1-S9 ESI†, collect bond distances and angles, atomic coordinates, anisotropic thermal parameters and hydrogen atom coordinates for **1** and **2**.

Table 2. Details of the crystal data, structural resolution and refinement procedure for **2** (synchrotron radiation on powdered sample).

Compound **2**	[Cu(PDC)((py)$_2$C(OH)$_2$)]
Formula	$C_{18}H_{13}N_3O_6Cu$
FW, g·mol^{-1}	430.85
Crystal system	Orthorhombic
Space group (no. 61)	*Pbca*
a, Å	7.4970(5)
b, Å	19.828(2)
c, Å	23.844(2)
V, Å^3	3544.5(4)
Z	8
ρ_{obs}, σ_{cal}, g·cm^{-3}	1.68(5), 1.687
F(000)	1752
μ, mm^{-1}	1.946
Synchrotron Radiation, λ, Å	0.8276(2)
Temperature, K	403.15(3)
No. of Points	3675
2θ (deg) interval	3.5–40.24
Refinement method	Full-matrix least-squares on F^2
Final *R* indices [I > 2σ(I)][a]	R_p = 0.050, R_{wp} = 0.065
R indices (all data)[a]	R_{exp} = 0.023, $R_{(F)}$ = 0.105
Goodness of fit on F^2	2.84
Parameters/restraints	114/95

[a]R1 = (Σw||F0| − |Fc||)/(Σw|F0|). wR2 = ((Σw((F0)^2 − (Fc)^2)^2)/((Σw((F0)^2)^2)$^{1/2}$. GOF = ((Σw((F0)^2 − (Fc)^2)^2)/((n − p))$^{1/2}$

Physicochemical characterization techniques.

Thermogravimetric analysis (TG) was performed in air atmosphere, up to 500 °C, with a heating rate of 5 °C min^{-1} on a DSC 2960 Simultaneous DSC-TGA TA Instrument. Thermodiffractometric analysis (TDX) was carried out in air atmosphere on a Brucker D8 Advance Vantec diffractometer (CuKα radiation), equipped with a variable-temperature stage (HTK2000) with Pt sample holder. The patterns were recorded each 10 °C from 30 to 350 °C (2θ step= 0.033, 2θ range = 8-38°, exposure time = 0.6 s, time measurement = 10 min).

The IR spectra were obtained with a Jasco FT/IR-6100 spectrophotometer in the 400–4000 cm^{-1} range with pressed KBr pellets. C, H and N elemental analyses were measured using a Euro EA 3000 Elemental analyzer.

Results and discussion

Crystal structure of compounds 1 and 2.

[Cu(PDC)((py)$_2$C(OH)$_2$)(H$_2$O)] (**1**) and [Cu(PDC)((py)$_2$C(OH)$_2$)] (**2**) are related through a reversible crystal-to-crystal transformation that will be explained below (section "Thermal analysis and structural transformation"), so they will be described together. In fact, both of them consist of monomers (Figures S1 and S2, ESI†) where the metal centre is coordinated to (N, O)-PDC and (N, N)-(py)$_2$C(OH)$_2$ ligands. This way, four equatorial positions are occupied around the metal ion in both compounds. For **2**, no other ligands can be found, so the coordination sphere is square-planar. For **1**, however, there is a single coordinated molecule of water completing a square pyramidal sphere. The Cu–O and Cu–N distances for **1** (Table S1, ESI†) lie within the ranges 1.949(2) Å–2.322(2) Å and 2.001(2) Å–2.021(2) Å, respectively. For **2** (Table S2, ESI†), the Cu–O distance is 1.96(2) Å and the Cu–N distances exhibit values between 1.92(2) Å–2.03(2) Å. The monomers form dimeric associations through hydrogen bonds (Tables S3 and S4, ESI†) between both organic ligands (Figure 1).

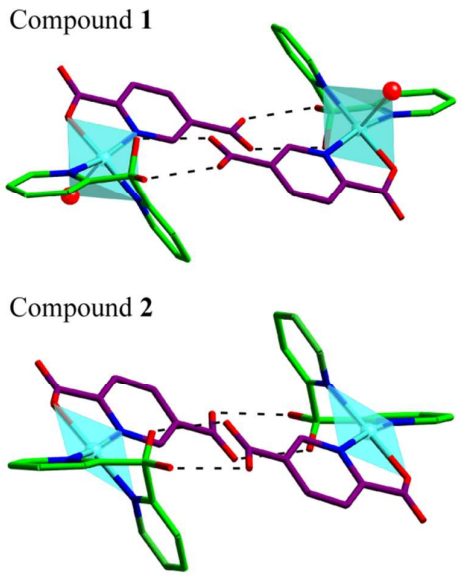

Figure 1. Dimeric associations for compounds **1** and **2**. Colour codes: Cu, turquoise; C(PDC), purple; C((py)$_2$C(OH)$_2$), green; N, blue and O, red (the oxygen corresponding to the coordinated molecule of water is the red ball). H-bonds are marked with black dotted lines. Hydrogen atoms are omitted for clarity.

The dimers are packed as shown in Figure 2. As observed, the packing is similar in both cases. However, the presence of the apical molecule of water in **1** allows the formation of hydrogen bonds with adjacent dimers through PDC ligands along the [100] direction, resulting in chains of dimers, and between these chains along the [001] direction, forming planes (Table S3, ESI†).

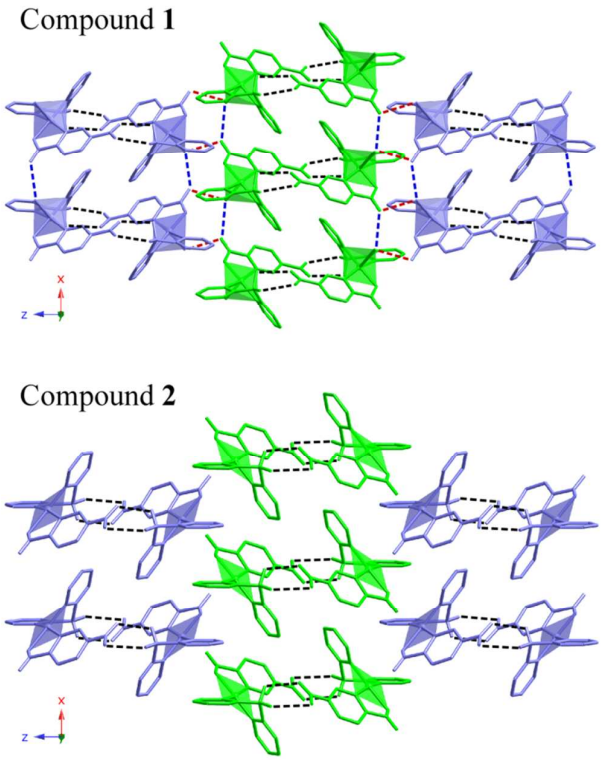

Figure 2. Packing of the dimers for compounds **1** and **2.** Hydrogen bonds are represented by dotted lines (black lines: intradimeric; blue lines: intrachain; red lines: interchain/intraplane).

The hydrogen bonds for compounds **1** and **2** have been analysed by graph-set.[49,50] While for **2** there is just a single type of hydrogen bonds resulting in a $R_2^2(8)$ assignment, for compound **1** there are three types of hydrogen bonds resulting in a DC(6)$R_2^2(8)$. As observed in Figure 2, the hydrogen bonds marked as dotted black lines are the most relevant as they produce the dimeric entities. The ones marked as blue and red dotted lines connect the dimers, and they are weaker.

Figure 3 shows a view of the whole framework where the wavy nature of the planes shown in Figure 2 can be seen. As observed, compound **2** shows sharper waves as a result of a significant compression of the framework (Tables 1 and 2) along the c direction (16.19%) in the absence of the coordinated molecule of water (c=28.4236(7) Å for **1** and c=23.844(2) Å for **2**). The b parameter, however, increases a 14.73% from b=17.2658(5) Å (for **1**) to 19.828(2) Å (for **2**). On the other hand, the change in a parameter is less significant (a=7.2953(2) Å for **1** and 7.4970(5) Å for **2**). As a result, there is a soft reduction of the unit cell volume (V=3580.2(2) Å^3 for **1** and V= 3544.5(5) Å^3 for **2**). In fact, if thinking of this system from **2** to **1**, it seems that molecules of water act as pins that alternatively push down the planes in opposite directions opening the angle formed by three consecutive chains (from 152.34° for **2** to 170.12° for **1**). As a consequence, the intradimeric Cu-Cu distances go from 9.023 Å (**2**) to 8.949 Å (**1**), the interchain ones from 5.042 Å (**2**) to 6.473 Å (**1**), and the interlayer ones from 9.021 Å (**2**) to 10.484 Å (**1**). That is, the presence/absence of single water molecule per metal ion provokes the framework to oscillate from open to close waves.

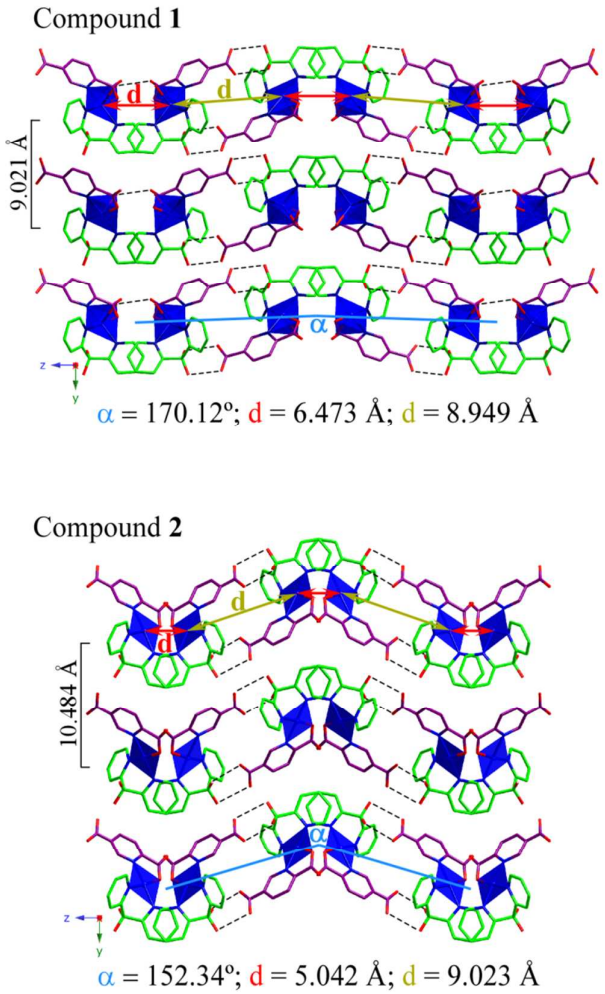

Figure 3. [100] view of the crystal structure for **1** and **2** showing intradimeric Cu-Cu distances (green arrow), interchain distance (red arrow), intralayer distance (black line) and interchain angle (blue line). Colour codes: Cu polyhedra, blue; C(PDC), purple; C((py)2C(OH)2), green; N, blue and O, red. H-bonds are marked with black dotted lines. Hydrogen atoms are omitted for clarity.

In summary, if taking into account the hydrogen bond system, compound **1** can be described as a 2D supramolecular framework, while compound **2** is 0D. Therefore, topological features for **1** were analyzed by means of TOPOS[51] software. The result is a uninodal 5-c net (Shubnikov {3^3;4^2}), shown in Figure S4, (ESI†).

Distortion of coordination spheres for metal complexes.

Distortion of coordination polyhedral was evaluated according to the Avnir[52,53] method, based on the continuous symmetry measures (CSM), using the SHAPE[54] program and the results can be seen in Table 3. Hypothetical compound $\mathbf{1_{SP}}$ has been also evaluated. Compound $\mathbf{1_{SP}}$ (square planar) is the result of manually removing the molecule of water in **1** (square pyramidal) for direct comparison with **2** (square planar). The projection of the as-calculated values on the distortion diagrams can be seen in Figures S5 and S6 (ESI†).

Table 3. Geometrical distortions of the trigonal bypiramid (TBPY) and Berry square pyramid (SPY) for **1**, and of the tetrahedron (D4h) and square (Td) for **2** and 1SP, calculated using SHAPE software.

	Pentacoordinate	*S*(*TBPY*)	*S*(*SPY*)
Compound **1**	Cu1	4.620	1.226
	Tetracoordinate	$S(D_{4h})$	$S(T_d)$
Compound **2**	Cu1	0.299	29.469
Compound $\mathbf{1_{SP}}$	Cu1	0.150	29.989

S= symmetry

As observed in Table 3, distortion for Cu^{II} sphere in **1** occurs v*ia* a non-Berry pathway that converts the trigonal bypiramid into a square pyramid[55] (SPY) with a soft contribution of a vacant octahedron (VOC) distortion. In fact, the axial distance (Cu1-OW = 2.322(2) Å) is longer than the equatorial ones (ranging from 1.949(2) Å to 2.021(2) Å). For compound **2**, the square planar Cu^{II} sphere exhibits a soft distortion occurring via the spread mode that traces the inter-conversion between the tetrahedron and the square.[55] In fact, bond distances in **2** lie in a narrow range (from 1.91(2) Å to 2.023(2) Å). For hypothetical compound $\mathbf{1_{SP}}$, there is higher distortion explained by the fact that bond angles are further from ideal (Tables S1 and S2, ESI†). This fact will be mentioned again below in the section "DFT calculations".

Thermal analysis and structural transformation.

Thermal analysis of **1** has been carried out by means of thermogravimetry (TG/DSC) and X-ray thermodiffractometry (TDX). TG analysis Figure S7 (ESI†) reveals that compound **1** suffers a mass loss of 4.55 % between 86°C and 125°C (approximately), which has been associated with the coordination molecule of water (4.01% calc.). The TG curve shows a stable plateau from 125°C to 155°C, and then a second mass loss takes place (76.85 %) up to 320°C. This second step has been assigned to the calcination of PDC and $(py)_2C(OH)_2$ molecules (78.26 % calc.). The final residue has been identified as CuO.[56]

A value of ΔH=44.67 kJ·mol^{-1} has been calculated from the DSC curve for the loss of the coordination water molecule. If considering that removal of a molecule of water implies the loss of two hydrogen bonds per metal ion in **1**, the calculated ΔH value is in agreement with the value of 21.5 kJ·mol^{-1} proposed by Wendler *et al*.[57] as the interaction energy per hydrogen bond involving coordinated molecules of water. It is worth mentioning that the value of 21.5 kJ·mol^{-1} do not correspond to a metal complex, so the similarity between values is outstanding.

Evidence of the existence of compound **2** was first detected from TG analysis, since the mass plateau along the TG curve (125°C-155°C) indicated the presence of a stable specimen. So, TDX diffractograms were collected on powdered sample from 30°C to 350°C at 10°C·min^{-1} (Figure S8, ESI†). The results indicated the occurrence of a phase transformation at approximately 100°C, yielding a crystalline product which is stable up to approximately 180°C. Upon further heating, the crystal structure collapses. This product was later identified to be compound **2**. With the main of acquiring more information about the **1**-to-**2** transformation, additional diffractograms were produced in 2°C steps from 80 °C to 120 °C (Figure 4). As observed, the formation of compound **2** starts about 95°C and finishes at 110 °C.

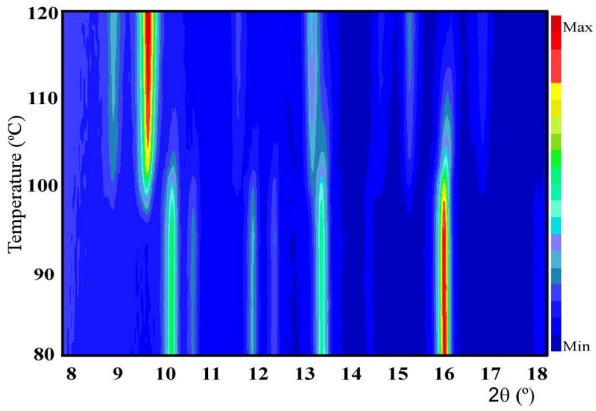

Figure 4. TDX diffractograms for **1** from 80 to 120 °C at 2 °C/min.

Several attempts were carried out in order to reproduce the **1**-to-**2** transformation on single crystal. However, the attempts were fruitless because single crystals do not keep integrity upon heating. On the other hand, elucidation of the crystal structure by powdered sample diffraction analysis was not possible with conventional X-ray because of the inadequate quality of the diffractograms (Figure S9, ESI†). This is the reason why synchrotron radiation has been used to elucidate the crystal structure of **2** (Figure S10, ESI†).

In order to have *in situ* images of the **1**-to-**2** transformation, several single crystals of compound **1** have been metalized for SEM analysis. A surface was selected and attacked by the microscope´s electron beam at different intensities (I) and exposures times with the aim of producing a local heating. Figure 5 shows the changes occurring on a fresh surface of **1** (I=1nA) after 30-second and 5-minute exposures. As observed, probably the electron beam provokes the **1**-to-**2** phase transformation, including the amorphisation of compound **2**. It is worth noticing that 30-second exposure at 40 nA produces the total collapse of the crystal.

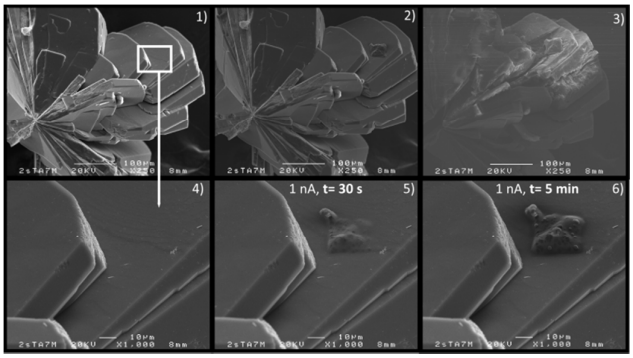

Figure 5. SEM images of the single-crystal surface of compound **1**. 1) fresh single crystal, 2) after 30-second exposure at 1nA, 3) after 5-minute exposure at 1nA, 4), 5) and 6) are details of images 1, 2 and 3, respectively.

Reversibility of the crystal-to-crystal transformation

The **1**-to-**2** crystal transformation detected by TDX analysis results in a color change of the sample from intense (**1**) to light (**2**) blue. The light tonality is kept upon cooling down to RT, indicating that **2** is stable at temperatures below its upon-heating formation temperature (95°C). However, this is a short-time stability because, after nine-minute exposure to the atmosphere at RT, the intense tonality is recovered, indicating the formation of **1**. Thus, soaking of **2** into water provokes immediately the light-to-intense color change. So, before knowing the crystal structure for **2**, we had evidence of the reversibility of the **1**-to-**2** transformation. It must be considered, that after elucidating it, it seems obvious that transformation is reversible but, prior to this, the color change was our first evidence.

In order to confirm reversibility of the transformation (**1**↔**2**), a powdered sample of **1** was heated to 130 °C (heating rate 15 °C min^{-1}) and then cooled down to RT. The as-cooled sample was determined to be compound **1** by means of FULLPROF pattern matching[58] of XRD diffractogram (Figure S11, ESI†) Additionally, upon-cooling TDX analysis was performed from 130 °C to 30 °C in 5 °C/min steps. As observed in Figure S12, ESI†, the formation of compound **1** starts at 50 °C but it coexists with compound **2** down to 35 °C. As previously said, the upon-heating formation of **2** starts at 95 °C, so the temperature divergence indicated the occurrence of thermal hysteresis. In order to evaluate it, diffraction peak areas were integrated (at 2θ=10.40° for **1** and 2θ=9.90° for **2**) by using the FIT mode of FULLPROF suite program[58] on XRD diffractograms collected from 30 to 130 °C and from 130 to 30 °C, at 5°C/min. The as-calculated values can be seen in Figure 6.

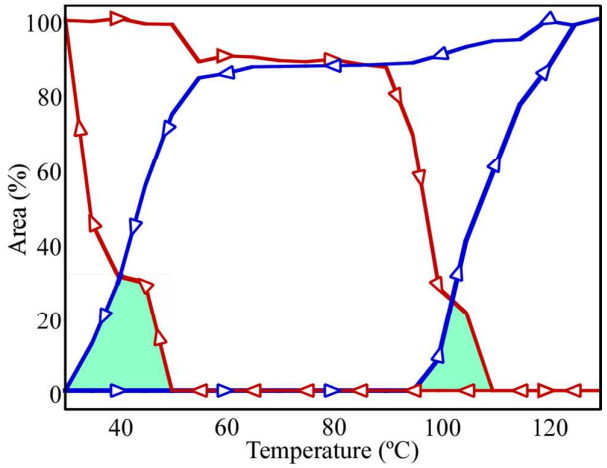

Figure 6. Hysteresis curves for **1** (red) and **2** (blue) under thermal treatment. Zone for phase coexistance is marked in green.

As observed in Figure 6, values of diffraction peak areas draw hysteresis curves for both compounds, and permit the easy identification of the thermal ranges for phase coexistance: 95-110 °C upon heating and 55-35 °C upon cooling.

DFT calculations

The fact that a single molecule of water provokes such a reversible transformation is possible because of the structural rearrangement. Taking into account that the loss of the coordinated molecule implies the disappearance of the hydrogen bond system that sustains the 2D array in **1**, the structural rearrangement producing **2** is expected to compensate it someway. Therefore, we decided to investigate the energetic aspects of the transformation by means of quantum-mechanical DFT calculations (Gaussian 03 program)[59] using Becke´s three parameter hybrid functional with the correlation functional of Lee, Yang and Parr (B3LYP)[60,61] and a split-valence basis set of 6-31G. Thus, we performed the calculations on the fragment shown in Figure 2, consisting of 14 monomeric units. Obviously, the fragment for **1** in Figure 2 contains 14 water molecules that were manually erased. In this way, direct comparison between $\mathbf{1_{SP}}$ and **2** was carried out. The results (Table S10 ESI†) show that **2** is more stable than $\mathbf{1_{SP}}$, in accordance with the experimental observations. Furthermore, a value of 5.4208493 Hartree (for the 14-unit fragment in figure 2) has been calculated for the energy difference between both selected fragments. So, even if the value is not representative of the whole network, it allows us to conclude that the structural rearrangement involves a high amount of energy. In other words, the role of the coordinated molecule of water exceeds the mere formation of hydrogen bonds. As explain above, the upon-cooling introduction of a single molecule of water into the square planar coordination sphere in **2** provokes a local, small distortion (explained above by comparison between $\mathbf{1_{SP}}$ and **2**) that extends through the whole framework. Upon heating, when water abandons **1**, there is a structural rearrangement that produces the stabilization of the structural units by the formation of **2**.

In the introduction we have mentioned other structural transformations in Cu^{II}-based SCFs involving coordinated and/or crystallization molecules of water that are removed/introduced or substituted.[40-42] Therefore, the transformation herein reported adds a new case characterized by its simplicity and effectiveness.

Conclusions

Among the diverse ways in which Cu^{II}-based SCFs can experiment crystal transformations, this work reports on one of the simplest ones, consisting of the removal/introduction of a single molecule of water into the coordination sphere of the metal ion. The as-provoked local, small distortion is magnified through the framework which responses by a complete structural rearrangement. This transformation is reversible producing an oscillation of the wavy planes.

Acknowledgements

This work has been financially supported by the "Ministerio de Economía y Competitividad" (MAT2013-42092-R), the "Gobierno Vasco" (Basque University System Research Group, IT-630-13) and UPV/EHU (UFI 11/15) which we gratefully acknowledge. SGIker (UPV/EHU) technical support is gratefully acknowledged. Authors thank Sergio Fernández for his support with SEM measurements. F. Llano-Tomé thanks the "Ministerio de Ciencia e Innovación" for a fellowship (BES-2011-045781).

Notes and references

1 H. Furukawa, K. E. Cordova, M. O'Keeffe and O. M. Yaghi, *Science,* 2013, **341**, 974.
2 M. O'Keeffe and O. M. Yaghi, *Chem. Rev,* 2012**, 112**, 675-702.
3 M. Li, D. Li, M. O'Keeffe and O. M. Yaghi, *Chem. Rev,* 2014**, 114**, 1343-1370.
4 T. R. Cook, Y. R. Zheng and P. J. Stang, *Chem. Rev,* 2013, **113**, 734-777.
5 F. Gandara, H. Furukawa, S. Lee and O. M. Yaghi, *J. Am. Chem. Soc,* 2014**, 136**, 5271-5274.
6 D. J. Tranchemontagne, K. S. Park, H. Furukawa, J. Eckert, C. B. Knobler and O. M. Yaghi, *J. Phys. Chem,* 2012**, 116**, 13143-13151.
7 T. A. Makal, J.-R. Li, W. Lu and H.-C. Zhou, *Chem. Soc. Rev,* 2012, **41**, 7761-7779.
8 S. R. Venna and M. A. Carreon, *Chem. Eng. Sci,* 2014, **120**, 174-190.
9 S. Chaemchuen, K. Zhou, N. A. Kabir, Y. Chen, X. Ke, G. Van Tendeloo and F. Verpoort, *Microporous Mesoporous Mater,* 2015, **201**, 277-285.
10 H. Jasuja, G. W. Peterson, J. B. Decoste, M. A. Browe and K. S. Walton, *Chem. Eng. Sci,* 2015, **124**, 118-124.
11 G. H. Dang, D. T. Nguyen, D. T. Le, T. Truong and N. T. S. Phan, *J. Mol. Catal. A Chem,* 2014, **395**, 300-306.
12 J. Liu, L. Chen, H. Cui, J. Zhang, L. Zhang and C.-Y. Su, *Chem. Soc. Rev,* 2014, **43**, 6011-6061.
13 D. Saha, T. Maity and S. Koner, *Dalton Trans,* 2014, **43**, 13006-13017.
14 Q. Hu, J. Yu, M. Liu, A. Liu, Z. Dou and Y. Yang, *J. Med. Chem,* 2014, **57**, 5679-5685.
15 J.-Q. Liu, J. Wu, Z.-B. Jia, H.-L. Chen, Q.-L. Li, H. Sakiyama, T. Soares, F. Ren, C. Daiguebonne, O. Guillou and S. W. Ng, *Dalton Trans,* 2014, **43**, 17265-17273.
16 M. C. Bernini, D. Fairen-Jimenez, M. Pasinetti, A. J. Ramirez-Pastor and R. Q. Snurr, *J. Mater. Chem, B* 2014**, 2**, 766-774.
17 X. Jiang, Y. Liu, P. Wu, L. Wang, Q. Wang, G. Zhu, X.-l. Li and J. Wang, *RSC Adv,* 2014, **4**, 47357-47360.
18 H. Liu, H. Wang, T. Chu, M. Yu and Y. Yang, *J. Mater. Chem. C,* 2014, **2**, 8683-8690.
19 J.-S. Guo, G. Xu, X.-M. Jiang, M.-J. Zhang, B.-W. Liu and G.-C. Guo, *Inorg. Chem,* 2014, **53**, 4278-4280.
20 P. Horcajada, T. Chalati, C. Serre, B. Gillet, C. Sebrie, T. Baati, J. F. Eubank, D. Heurtaux, P. Clayette, C. Kreuz, J.-S. Chang, Y. K. Hwang, V. Marsaud, P.-N. Bories, L. Cynober, S. Gil, G. Ferey, P. Couvreur and R. Gref, *Nat. Mater,* 2010, **9**, 172-178.
21 P. Horcajada, R. Gref, T. Baati, P. K. Allan, G. Maurin, P. Couvreur, G. Ferey, R. E. Morris and C. Serre, *Chem. Rev,* 2012, **112**, 1232-1268.
22 E. Coronado, M. Gimenez-Marques and G. Minguez Espallargas, *Inorg. Chem,* 2012, **51**, 4403-4410.
23 R. Fernandez de Luis, J. Orive, E. S. Larrea, M. K. Urtiaga, M. I. Arriortua, *Cryst. Growth Des,* 2014, **14**, 658-670.
24 S.-Y. Ke, Y.-F. Chang, H.-Y. Wang, C.-C. Yang, C.-W. Ni, G.-Y. Lin, T.-T. Chen, M.-L. Ho, G.-H. Lee, Y.-C. Chuang and C.-C. Wang, *Cryst. Growth Des,* 2014, **14**, 4011-4018.
25 G. K. Kole, J. J. Vittal, *Chem. Soc. Rev,* 2013, **42**, 1755-1775.
26 D. Froehlich, S. K. Henninger and C. Janiak, *Dalton Trans,* 2014, **43**, 15300-15304.
27 A. Calderon-Casado, G. Barandika, B. Bazan, M. K. Urtiaga and M. I. Arriortua, *CrystEngComm,* 2010, **12**, 1784-1789.
28 A. Calderon-Casado, G. Barandika, B. Bazan, M. K. Urtiaga, O. Vallcorba, J. Rius, C. Miravittles and M. I. Arriortua, *CrystEngComm,* 2011, **13**, 6831-6838.
29 A. Calderon-Casado, G. Barandika, B. Bazan, M. K. Urtiaga and M. I. Arriortua, *CrystEngComm,* 2013, **15**, 5134-5143.
30 M. I. Arriortua Marcaida, M. G. Barandika Argoitia, B. d. P. Bazan Blau, A. Calderon Casado and M. K. Urtiaga Greaves, Alcohol and water sensor compounds, detection method and device. Patent: PCT Int. Appl., *WO 2013057350 A1.*
31 F. Llano-Tome, B. Bazan, M. K. Urtiaga, G. Barandika, L. Lezama and M. I. Arriortua, *CrystEngComm,* 2014, **16**, 8726-8735.
32 G. S. Papaefstathiou, A. Escuer, F. A. Mautner, C. Raptopoulou, A. Terzis, S. P. Perlepes and R. Vicente, *Eur. J. Inorg. Chem,* 2005, 879-893.
33 B. F. Abrahams, T. A. Hudson and R. Robson, *Chem. Eur. J,* 2006, **12**, 7095-7102.
34 C. G. Efthymiou, C. Papatriantafyllopoulou, G. Aromi, S. J. Teat, G. Christou and S. P. Perlepes, *Polyhedron,* 2011, **30**, 3022-3025.
35 Z. Serna, M. G. Barandika, R. Cortes, M. K. Urtiaga and M. I. Arriortua, *Polyhedron,* 1998, **18**, 249-255.
36 M. G. Barandika, R. Cortes, Z. Serna, L. Lezama, T. Rojo, M. K. Urtiaga and M. I. Arriortua, *Chem. Commun,* 2001, 45-46.
37 Z. E. Serna, R. Cortes, M. K. Urtiaga, M. G. Barandika, L. Lezama, M. I. Arriortua and T. Rojo, *Eur. J. Inorg. Chem,* 2001, 865-872.
38 M. G. Barandika, Z. E. Serna, M. K. Urtiaga, J. I. R. De Larramendi, M. I. Arriortua and R. Cortes, *Polyhedron,* 1999, ***18***, 1311-1316.
39 P. Diaz-Gallifa, O. Fabelo, L. Canadillas-Delgado, J. Pasan, A. Labrador, F. Lloret, M. Julve and C. Ruiz-Perez, *Cryst. Growth Des,* 2013, **13**, 4735-4745.
40 X. Yang, J. D. Ranford and J. J. Vittal, *Cryst. Growth Des,* 2004, **4**, 781-788.
41 T. Washizaki, R. Ishikawa, K. Yoneda, S. Kitagawa, S. Kaizaki, A. Fuyuhiro and S. Kawata, *RSC Adv,* 2012, **2**, 12169-12172.

42 Y.-M. Jiang, Z. Yin, K.-H. He, M.-H. Zeng and M. Kurmoo, *Inorg. Chem,* 2011, **50**, 2329-2333.
43 L. Bravo-García, G. Barandika, B. Bazán, M. K. Urtiaga and M. I. Arriortua, *Polyhedron*, 2015, **92**, 117-123.
44 P. Roman and J. M. Gutierrez-Zorrilla, *J. Chem. Educ,* 1985, **62**, 167-168.
45 W. Yinghua, *J. Appl. Crystallogr,* 1987, ***20***, 258-259.
46 A. Altomare, G. Cascarano, C. Giacovazzo and A. Guagliardi, *J. Appl. Crystallogr,* 1993, ***26***, 343-350.
47 G. M. Sheldrick, *Acta Crystallogr., Sect. A Found. Crystallogr,* 2008, **64**, 112-122.
48 V. Petricek, M. D. a. L. P., *The crystallographic Computing System, Institute of Physics, Praha, Czech Republic,* 2006.7
49 M. C. Etter and J. C. MacDonald, *Acta Cryst*, 1990, **B46**, 256-262.
50 J. Bernstein, R. E. Davis, L. Shimoni and N-L. Chang, *Angew. Chem. Int. Ed. Engl*, 1995, **34**, 1555-1573.
51 V. A. Blatov, A. P. Shevchenko and D. M. Proserpio, *Cryst. Growth Des,* 2014, **14**, 3576-3586.
52 H. Zabrodsky, S. Peleg and D. Avnir, *J. Am. Chem. Soc,* 1992, **114**, 7843-7851.
53 M. Pinsky and D. Avnir, *Inorg. Chem,* 1998, **37**, 5575-5582.
54 M. Llunel, D. C., J. Cirera, J. M. Bofill, P. Alemany, S. Álvarez, M. Pinsky and D. Yanutir, SHAPE v1.1a, 2003, Program for continuous shape measure calculation of polyhedral Xn and MLn fragments, http://www.ee.ub.edu/.
55 S. Alvarez, P. Alemany, D. Casanova, J. Cirera, M. Llunell, D. Avnir, *Coord. Chem. Rev,* 2005, **249**, 1693-1708.
56 B. Liu, L. Wei, N.-n. Li, W.-P. Wu, H. Miao, Y.-Y. Wang and Q.-Z. Shi, *Cryst. Growth Des,* 2014, **14**, 1110-1127.
57 K. Wendler, J. Thar, S. Zahn and B. Kirchner, *J. Phys. Chem. A,* 2010, **114**, 9529-9536.
58 M. G. Barandika, M. L. Hernandez-Pino, M. K. Urtiaga, R. Cortes, L. Lezama, M. I. Arriortua and T. Rojo, *Dalton,* 2000, **9**, 1469-1473.
59 M. J. Frisch, G. W. Trucks, H. B. Schlegel, G. E. Scuseria, M. A. Robb, J. R. Cheeseman, J. A. Montgomery, J. T. Vreven, K. N. Kudin, J. C. Burant, J. M. Millam, S. S. Iyengar, J. Tomasi, V. Barone, B. Mennucci, M. Cossi, G. Scalmani, N. Rega, G. A. Petersson, H. Nakatsuji, M. Hada, M. Ehara, K. Toyota, R. Fukuda, J. Hasegawa, M. Ishida, T. Nakajima, Y. Honda, O. Kitao, H. Nakai, M. Klene, X. Li, J. E. Knox, H. P. Hratchian, J. B. Cross, V. Bakken, C. Adamo, J. Jaramillo, R. Gomperts, R. E. Stratmann, O. Yazyev, A. J. Austin, R. Cammi, C. Pomelli, J. W. Ochterski, P. Y. Ayala, K. Morokuma, G. A. Voth, P. Salvador, J. J. Dannenberg, V. G. Zakrzewski, S. Dapprich, A. D. Daniels, M. C. Strain, O. Farkas, D. K. Malick, A. D. Rabuck, K. Raghavachari, J. B. Foresman, J. V. Ortiz, Q. Cui, A. G. Baboul, S. Clifford, J. Cioslowski, B. B. Stefanov, G. Liu, A. Liashenko, P. Piskorz, I. Komaromi, R. L. Martin, D. J. Fox, T. Keith, M. A. Al-Laham, C. Y. Peng, A. Nanayakkara, M. Challacombe, P. M. W. Gill, B. Johnson, W. Chen, M. W. Wong, C. Gonzalez and J. A. Pople, *GAUSSIAN 03, (Revision D.02)*. Gaussian, Inc., Wallingford CT, 2004.
60 A. D. Becke, *J. Chem. Phys,* 1993, **98**, 5648-5652.
61 C. Lee, W. Yang and R. G. Parr, *Phys. Rev. B Condens. Matter,* 1988, **37**, 785-789.

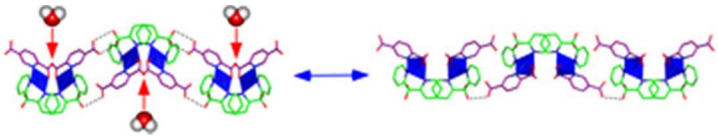

Water-induced reversible phase transformation in the CuII-PDC-(py)2C(OH)2 system
30x5mm (300 x 300 DPI)